Int. J. Solids Structures, 1975, Vol. 11, pp. 777–791. Pergamon Press. Printed in Great Britain.

EFFECTS OF PHASE GEOMETRY AND VOLUME FRACTION ON THE PLANE STRESS LIMIT ANALYSIS OF A UNIDIRECTIONAL FIBER-REINFORCED COMPOSITE†

SAURINDRANATH MAJUMDAR‡
Assistant Mechanical Engineer, Materials Science Division, Argonne National Laboratory, Argonne, IL 60439, U.S.A.

and

P. V. MCLAUGHLIN, JR.‡
Senior Engineer, Materials Sciences Corporation, Merion-Towle Building, Blue Bell Office Campus, Blue Bell, PA 19422, U.S.A.

(*Received* 7 *January* 1974; *revised* 2 *June* 1974)

Abstract—Limit theorems of plasticity are applied to unidirectional fiber-reinforced composite materials to determine bounds to plastic limit conditions for the composite in average stress space. For this purpose a representative volume element (RVE), sufficiently large compared to the scale of inhomogenity of the composite, is chosen and analyzed by limit analysis methods.

Upper and lower bounds to the plane average stress limit condition for the composite are derived for the following geometries which are presented in descending order of generality.

(a) Only volume fraction of phases are known.
(b) Volume fraction and fiber cross-section shape are known, but the size and distribution are arbitrary.
(c) Deterministic periodic array.

The bounds are shown to be improved at the cost of generality of fiber geometry and distribution. An evaluation is made of the effects of fiber volume fraction and distribution geometry on the composite limit condition.

1. INTRODUCTION

Limit analysis of plasticity appears to have been first used to determine strengths of composite materials by Drucker [1]§ who computed the limit load in simple tension of a material consisting of ideally plastic matrix and rigid particles. Hashin [2] employed the same method for computing transverse limit strength of fiber-reinforced composite materials. Drucker [3] computed the limit load of a two dimensional composite consisting of rigid equal hexagonal fibers regularly arranged and embedded in an ideally plastic matrix for the limiting case of very small volume fraction of fibers. Butler and Sullivan [4] have obtained bounds for transverse strength of similar composites. Shu and Rosen [5] used the limit analysis theorems to bound limit loads for uniaxial fiber-reinforced materials described by the composite cylinder assemblage model for various cases of loadings. Prager [6] considered the specific case of reinforcement of a rigid-plastic Von Mises matrix with one and two families of filaments having infinitesimal cross-section but infinite strength. Helfinstine and Lance [7] attempted a similar analysis for a matrix material obeying the Tresca criterion. McLaughlin [8] developed a method for determining the limit condition in average plane stress space for a matrix having any limit condition, and reinforced by any number of fiber families. While the fibers in [8] could be either plastic or rigid, the analysis was applicable only for very small volume fraction of high strength fibers. Majumdar [9] and Majumdar and McLaughlin [10] have discussed the validity of using limit analysis techniques to determine limit strengths for composite materials in terms of average stresses, and have discussed limitations of the application thereof to limit analysis of composite structures.

The present paper considers the plane stress limit conditions for unidirectional fiber-reinforced composites having various phase geometry and volume fractions of fibers and

†Based in part on a thesis submitted to the University of Illinois by the first author in partial fulfillment of the requirement of the degree of Doctor of Philosophy.

‡Formerly Assistant Professor, Department of Theoretical and Applied Mechanics, University of Illinois at Urbana-Champaign.

§Numbers in square brackets indicate references at the end of the paper.

assumes each phase to be homogeneous, isotropic and elastic-plastic with a limit condition. Using the limit theorems of plasticity[11] upper and lower bounds to the plane stress limit conditions are obtained for (a) the most general case of knowledge of volume fractions alone, (b) the more restricted case where the cross-sectional shape of fibers are known but size and distribution are arbitrary, and (c) several types of periodic arrays of fibers with known cross-sections. Comparisons are made between the bounds for various cases showing effects of volume fraction of fibers and geometry on the plane stress limit condition for unidirectional fiber-reinforced composites.

The results reported here are not applicable to the important practical case of a composite material reinforced by brittle fibers. However, for most high strength brittle fiber-reinforced composites where the elastic modulus of the fiber is much larger than that of the matrix, the assumption of rigid fiber in limit analysis of the composite is reasonable.

2. IDEALIZATION OF COMPOSITE GEOMETRY

The geometry of any composite material involves not only the size and shape of each of the phases but also how these phases are distributed with respect to one another. When a large number of phase "particles" are non-uniformly distributed in a composite, it becomes impractical to try to define the size and location of each of the constituent "particles". A representative volume element (RVE) is then chosen to encompass a sufficient number of these different phases so that macroscopic homogeneity guarantees that the average properties of each of these RVE's are the same. In order to analyze the RVE, however, some geometrical information is necessary. If the phases are distributed at random, a statistical description as given by Frisch[19] might be adopted. This description has been used by Hashin[13], and Beran[14] to determine bounds to the average elastic constants of composites. However, in many practical applications, such as unidirectional fiber reinforced composites, the fiber distribution is not completely random. In certain fibrous composites the fiber distribution has an approximately periodic nature and in such cases a perfectly periodic array (such as hexagonal or rectangular array) may be a useful model. In this way the geometry of the RVE becomes completely deterministic.

One important set of geometric parameters is the volume fractions of the constituent phases which are also the first order statistics of the random medium. In many composites this is the only information that is available with some accuracy. A desirable objective then would be to obtain the best possible bounds to the limit condition for the composite from a knowledge of the volume fraction of phases alone. Such bounds may, of course, be expected to be wide apart. If more information than the volume fraction is available, better bounds to the limit condition should be obtainable.

The present paper deals only with unidirectional fiber-reinforced composites with the fibers aligned in the x_1 direction (Fig. 1). The following are the geometries considered here in terms of descending order of generality:

(1) Only volume fraction of phases are known. Nothing is known about the fiber shape, size or distribution. This is the most general situation with a minimum of geometrical data available.

(2) Volume fractions and fiber cross-sectional shapes are known, but the size and distribution of fibers are arbitrary.

(3) Lastly, two types of deterministic periodic arrays of fibers hexagonal and rectangular (Fig. 1), are analyzed. Because of the periodicity of the accompanying stress and strain rate fields, it is sufficient to consider a unit cell as the RVE.

3. UPPER AND LOWER BOUNDS TO THE LIMIT CONDITION IN GENERALIZED PLANE STRESS SPACE

An upper bound[9] to the composite limit condition is obtained by assuming any compatible collapse velocity field in the RVE and equating the resulting dissipation rate to the external work rate by the average surface tractions on the surface of the RVE. A lower bound[9] to the composite limit condition is obtained by assuming any equilibrium stress field which is everywhere at or below respective local phase limit-conditions, and then computing the corresponding average stresses.

It should be noted that even though the results obtained here are for fibers aligned in the x_1 direction, they can be generalized to include cases where the fibers are at any arbitrary angle to

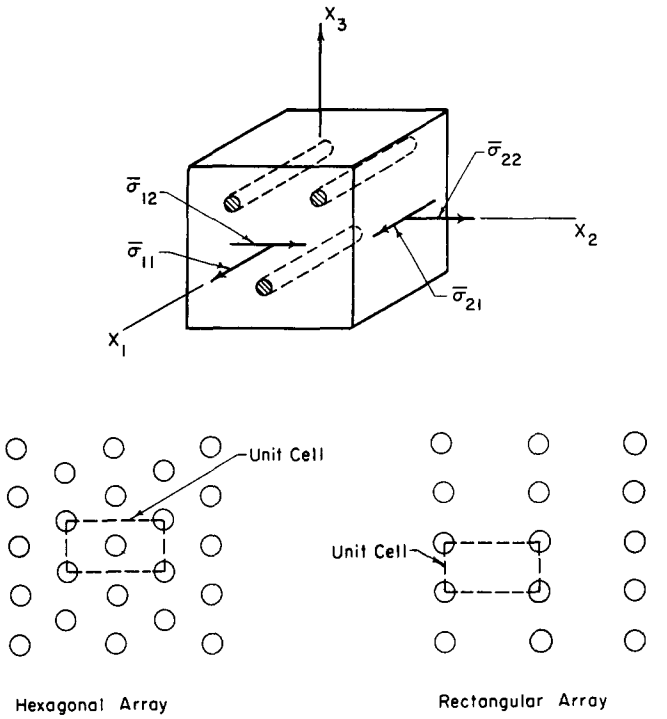

Fig. 1. Typical loading and fiber arrays for unidirectional fiber-reinforced composite RVE.

the x_1 direction by means of the transformation equations of plane stress. Also these results may be used for fiber-reinforced plates loaded in plane average stress provided the number of layers of fibers through the thickness are large so that there is no "thickness effect".

3.1 *Only volume fractions are known*

Upper bound. A collapse velocity is assumed such that the strain rate field is a constant, $\bar{\epsilon}_{\alpha\beta}$, throughout the RVE. It can be shown that the resulting upper bound to the average or effective composite limit stress, $\bar{\sigma}^{UB}_{\alpha\beta}$, is

$$\bar{\sigma}^{UB}_{\alpha\beta} = v_F \sigma^F_{\alpha\beta} + v_M \sigma^M_{\alpha\beta}, (\alpha, \beta = 1, 2) \tag{3.1}$$

where $\sigma^F_{\alpha\beta}$ and $\sigma^M_{\alpha\beta}$ are the fiber and the matrix stresses corresponding to the strain rate $\bar{\epsilon}_{\alpha\beta}$ (Fig. 2a) respectively. This upper bound surface can be constructed by adding the volume fraction weighted stresses of the matrix and the fiber from points on the respective limit conditions having the same outer normal. If the fibers were infinitely rigid, this upper bound surface would recede to infinity.

Given only the volume fractions, equation (3.1) gives the best upper bound possible in the $\bar{\sigma}_{11}$, $\bar{\sigma}_{22}$, $\bar{\sigma}_{12}$ space. This can be shown by considering the special geometry in Fig. 2b where the volume fraction v_F of the fibers is distributed as plates lying parallel to the $x_1 - x_2$ plane. For this specific geometry $\sigma^F_{\alpha\beta}$ and $\sigma^M_{\alpha\beta}$ as defined above represent a statically admissible stress field, and consequently a lower bound to the composite limit condition is $\bar{\sigma}^{LB}_{\alpha\beta} = v_F \sigma^F_{\alpha\beta} + v_M \sigma^M_{\alpha\beta}$. Since the upper and lower bounds coincide, they represent the exact limit condition for this special geometry. Equation (3.1) gives the best possible upper bound from a knowledge of volume fraction alone because if it were possible to reduce this upper bound, then, in particular, the reduction would also apply to the geometry of Fig. 2b. This is clearly impossible since equation (3.1) is the exact limit condition for this special geometry.

It should be noted that equation (3.1) can easily be generalized to include an n-phase composite material of arbitrary phase geometry. This has been discussed by Hashin[15] for the special case where all phases are made of Von Mises material.

Lower bound. Since the fibers are prismatic and aligned in the x_1 direction, a discontinuity in the σ_{11} component of the stress tensor is permissible at the fiber-matrix interface. Hence, for

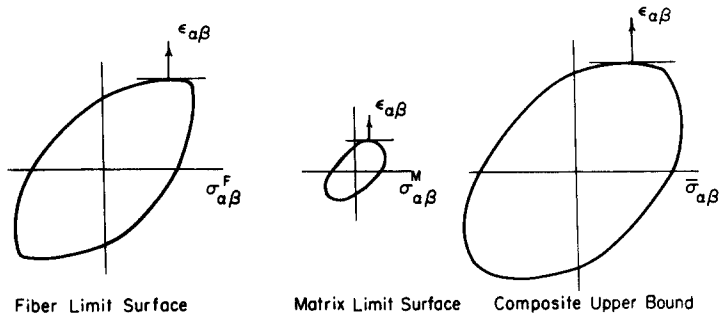

(a) Construction of General Upper Bound

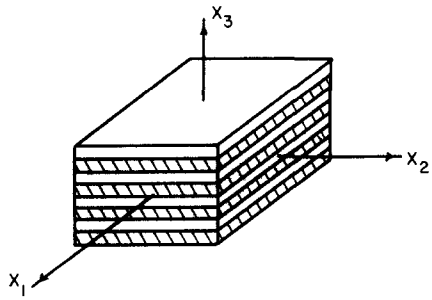

(b) Special Geometry for which General Upper Bound is Exact Plane Limit Condition

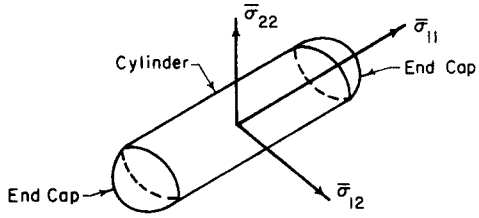

(c) Schematic of General Lower Bound

Fig. 2. General upper and lower bounds.

constructing a lower bound, the following statically admissible piecewise constant stress field is assumed

$$\sigma^F_{11} = \sigma^M_{11} + \sigma,\ \sigma^F_{22} = \sigma^M_{22},\ \sigma^F_{12} = \sigma^M_{12} \tag{3.2}$$

such that

$$L^M(\sigma^M_{\alpha\beta}) = 0, \text{ and } L^F(\sigma^F_{\alpha\beta}) \leq 0. \tag{3.3 and 3.4}$$

The superscripts F and M refer to fiber and matrix respectively, L is the individual phase limit condition and σ is a constant to be chosen later to maximize the lower bound. A lower bound to the composite limit condition $\bar{\sigma}^{LB}_{\alpha\beta}$, is then given by

$$\bar{\sigma}^{LB}_{11} = \sigma^M_{11} v_M + \sigma^F_{11} v_F,\ \bar{\sigma}^{LB}_{22} = \sigma^M_{22},\ \bar{\sigma}^{LB}_{12} = \sigma^M_{12}. \tag{3.5}$$

Solving for the matrix stresses in terms of $\bar{\sigma}^{LB}_{\alpha\beta}$ and σ, and substituting them into the matrix limit condition (equation 3.3) gives

$$L^M[(\bar{\sigma}^{LB}_{11} - \sigma v_F),\ \bar{\sigma}^{LB}_{22},\ \bar{\sigma}^{LB}_{12}] = 0 \tag{3.6}$$

Similarly, solving for the fiber stresses in terms of $\bar{\sigma}^{LB}_{\alpha\beta}$ and σ, and substituting them into the fiber limit condition (equation 3.4) gives

$$L^F[(\bar{\sigma}^{LB}_{11} + \sigma v_M),\ \bar{\sigma}^{LB}_{22},\ \bar{\sigma}^{LB}_{12}] \leq 0 \tag{3.7}$$

Since the fiber is assumed much stronger than the matrix, there will be some combination of the applied lower bound stresses for which the matrix stresses will be at the limit-condition but the fiber stresses will be contained within the fiber limit condition, i.e. the inequality in (equation 3.4) will be satisfied. In such situations the value of σ can be chosen so as to maximize the lower bound. This is achieved by solving for σ from the following equations simultaneously

$$\partial \bar{\sigma}_{\alpha\beta}^{LB}/\partial\sigma = 0$$
$$\partial L^{M}[(\bar{\sigma}_{11}^{LB} - \sigma v_F), \bar{\sigma}_{22}^{LB}, \bar{\sigma}_{12}^{LB}]/\partial\sigma = 0.$$

The resulting value of σ is then substituted into equation (3.6) to give lower bound to that portion of the composite limit condition which satisfies the inequality 3.7. Outside this range, the fiber stresses are at the limit condition and the equality in equation (3.7) has to be satisfied. σ has then to be obtained from solving equations (3.6) and (3.7) simultaneously. This value of σ when substituted into either of equations (3.6) and (3.7) gives the remaining portion of the lower bound to the composite limit condition. Note that the procedure given here for determining a lower bound to the composite limit condition is applicable to arbitrarily distributed fibers of any cross-sectional shape and to cases where the fiber and matrix obey different limit conditions.

Detailed calculations have been carried out for the case where both the fiber and the matrix obey the Von Mises limit condition, and σ_F and σ_M are their respective uniaxial limit strength with $\sigma_F > \sigma_M$ [9]. Only the final results are presented here. The portion of the lower bound which corresponds to the fiber stress below limit condition is, as might be expected, the plane strain matrix limit condition and consists of an elliptic cylinder whose axis is in the $\bar{\sigma}_{11}$ direction (Fig. 2c). The equation for the cross-section of the cylinder is the ellipse

$$\bar{\sigma}_{22}^{LB^2} + 4\bar{\sigma}_{12}^{LB^2} = \frac{4}{3}\sigma_M^2. \tag{3.8}$$

This cylinder is a valid lower bound between the pair of parallel planes given by

$$2\bar{\sigma}_{11} - \bar{\sigma}_{22} = \pm 2v_F(\sigma_F^2 - \sigma_M^2)^{1/2}. \tag{3.9}$$

Beyond these parallel planes the cylinder is closed by end caps, corresponding to fiber stresses at limit, whose equations are

$$[(v_M - v_F)\bar{L} + (\sigma_F v_F)^2 - (\sigma_M v_M)^2] \pm (2\bar{\sigma}_{11}^{LB} - \bar{\sigma}_{22}^{LB})[v_M v_F \bar{L} - v_F(\sigma_M v_M)^2 - v_M(\sigma_F v_F)^2]^{1/2} = 0 \tag{3.10}$$

where

$$\bar{L} = \bar{\sigma}_{11}^{LB^2} + \bar{\sigma}_{22}^{LB^2} - \bar{\sigma}_{11}^{LB}\bar{\sigma}_{22}^{LB} + 3\bar{\sigma}_{12}^{LB^2}.$$

The end caps recede further and further as the fiber limit strength is increased. In the limit when the fibers are infinitely strong, the lower bound reduces to the infinite cylinder given by equation (3.8).

The lower bound and the upper bound coincide for uniaxial tension $\bar{\sigma}_{11}$ loading and therefore they represent the exact limit strength, i.e. $\bar{\sigma}_{11}^{L} = \sigma_F v_F + \sigma_M v_M$.

It is difficult to conclude that the general lower bound obtained here is the best possible from a knowledge of volume fraction alone. This conclusion can, however, be reached for the transverse tension ($\bar{\sigma}_{22}$) or the in-plane shear ($\bar{\sigma}_{12}$) loading[9].

For stress states other than simple tension in the fiber direction, simple tension transverse to the fiber direction, and pure in-plane shear, exact limit conditions have not been found which coincide with the general lower bound as given by equations (3.8) and (3.10). These equations may, therefore, not represent the best possible lower bound to the limit condition under a general combined plane stress loading from the knowledge of volume fraction alone.

In the case where only volume fraction of fibers are known, the upper bound to the composite limit condition corresponding to equation (3.1) may be far greater than the lower bound corresponding to equations (3.8) and (3.10) for practical values of fiber strength and volume

fraction. Only when the volume fraction of fibers is very small, so that the volume fraction weighted uniaxial limit strengths of the fiber and matrix are comparable ($v_F\sigma_F \approx v_M\sigma_M$), these may yield reasonable bounds. An example is shown in Fig. 3a where the ratio of the volume fraction weighted uniaxial strengths of the fiber and the matrix is unity, i.e. $v_F\sigma_F = v_M\sigma_M$.

The general lower bounds given by equations (3.8) and (3.10) can be shown to reduce to the "exact" limit condition for infinitesimal fiber-reinforced composites given by McLaughlin[8] if the following limit is imposed on the lower bound solution:

$$v_F \to 0,\ \sigma_F \to \infty,\ v_F\sigma_F \to \text{Finite}.$$

The lower bound and the infinitesimal fiber limit condition coincide in the $\bar{\sigma}_{22} - \bar{\sigma}_{12}$ space for all v_F (equation 3.8). Fig. 3b shows the comparison between the infinitesimal fiber limit condition and the lower bound for finite volume fraction of fibers in the $\bar{\sigma}_{11} - \bar{\sigma}_{12}$ and $\bar{\sigma}_{11} - \bar{\sigma}_{22}$ spaces for various v_F and σ_F/σ_M values. It is seen that the infinitesimal fiber condition is very close to the lower bound for finite volume fraction of fibers especially for large ratios between the fiber and the matrix uniaxial strengths. In all cases the infinitesimal fiber condition is a valid lower bound for the true composite limit condition.

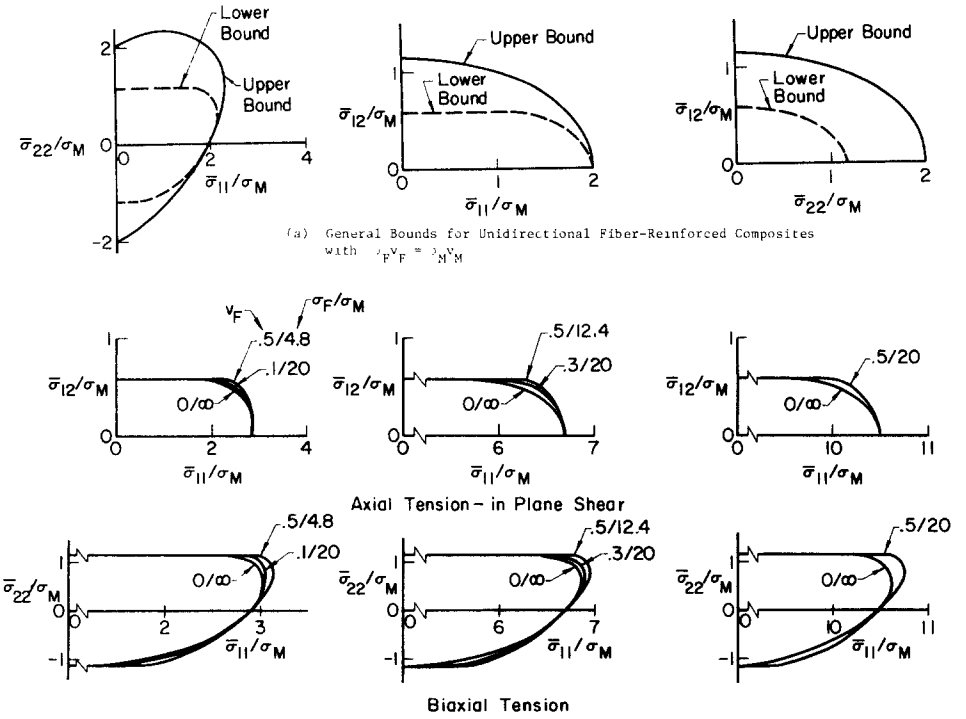

(a) General Bounds for Unidirectional Fiber-Reinforced Composites with $v_F\sigma_F = v_M\sigma_M$

(b) Comparison of General Lower Bounds with Infinitesimal Fiber Limit Conditions

Fig. 3. General upper and lower bounds.

3.2 *Volume fraction and cross-section shape are known circular cylindrical fibers*

Upper bound. If, in addition to volume fraction, the fiber cross-sectional shape is known, it is possible to reduce the upper bound to the in-plane shear limit strength[16]. For the present the fiber cross-sections are assumed to be circles with varying diameter and distributed arbitrarily in the $x_2 - x_3$ plane (Fig. 4a). The collapse velocity field for the ith cylinder is assumed in the following form

$$u_1 = \begin{cases} 2\bar{\epsilon}_{12}\, r_i \cos\theta_i & \text{for } |r - r_i| < a_i \\ 2\bar{\epsilon}_{12}\, r \cos\theta & \text{for } |r - r_i| > a_i \end{cases}$$

$$u_2 = u_3 = 0.$$

This corresponds to zero strain rate in the fibers and a strain rate field in the matrix of

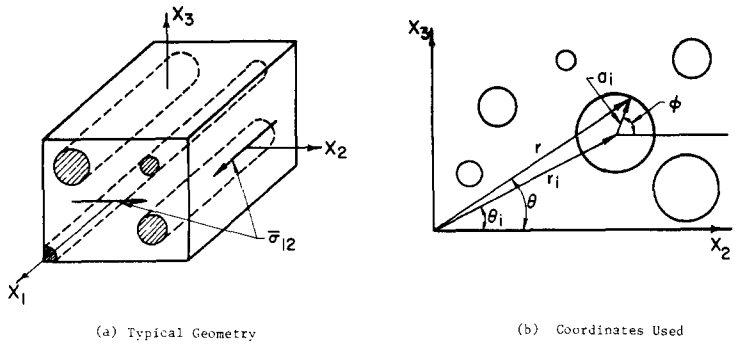

Fig. 4. Geometry and coordinates for circular section fiber-reinforced composite.

$\epsilon_{1r} = \bar{\epsilon}_{12} \cos\theta$, $\epsilon_{1\theta} = -\bar{\epsilon}_{12} \sin\theta$. In addition, there is a tangential velocity discontinuity at the fiber-matrix interface whose magnitude is $|2\bar{\epsilon}_{12}\, a_i \cos\phi|$ (Fig. 4b). Equating the external work rate to the internal dissipation rate for the assumed collapse field,

$$\bar{\sigma}_{12}^{UB}/k = 1 + (4/\pi - 1)v_F \tag{3.11}$$

where k is the limit strength of the matrix in shear. Note that this upper bound to the in-plane shear strength of the composite is independent of the fiber limit strength.

Shu and Rosen[5] obtained similar upper bounds to the shear strength of unidirectional fiber-reinforced composites from a knowledge of volume fraction and circular cross-section of the fibers. Their result is compared with that given by equation (3.11) in Table 1. It is seen that equation (3.11) provides significant improvement over Shu and Rosen's[5] especially for large volume fractions of fibers. An interesting consequence of equation (3.11) is that using circular section fibers, the limit shear strength of a unidirectional fiber-reinforced composite can at most be increased by 27 per cent above the matrix shear strength no matter what volume fraction or distribution of fiber is used.

Table 1. Upper bounds to in-plane shear strength of uniaxial fiber-reinforced composite

Volume fraction	Upper Bound According to	
	Shu and Rosen [5]	Eq. 3.11
.25	1.1427	1.0683
.49	1.2797	1.1339
.81	1.4623	1.2213
.9025	1.5151	1.2466

Lower bound. The lower bounds derived in Section 3.1 for arbitrary fiber cross-section and location are also applicable to composites with known fiber cross-section. For circular fibers with arbitrary size and location, these bounds could not be improved. In fact, these lower bounds to the limit strength in transverse tension and in-plane shear for arbitrary fiber cross-section and location are the best possible lower bounds from a knowledge of volume fraction and circular cross-sectional shape of the fibers only[9]. Thus, equation (3.8) gives the best possible lower bounds to the transverse strength ($\bar{\sigma}_{12}^{LB} = 0$) and in-plane shear strength ($\bar{\sigma}_{22}^{LB} = 0$) of circular section fiber-reinforced composites where only volume fraction is additionally known.

3.3 *Periodic array*

Upper bound. If the exact geometry of the RVE is known, it is possible to improve the upper bound to the average limit condition significantly. This is made possible because the internal dissipation rate can be reduced considerably by choosing discontinuous velocity fields that do not produce any strain rate in the fibers. Obviously such velocities will depend very strongly on the exact geometry of the RVE. For the present, only the general hexagonal and rectangular array (Fig. 1) of circular section fibers, each of radius a, are chosen, and both the matrix and the fiber materials are assumed to obey the Von-Mises limit condition. For this assumed geometry various

modes of collapse are permissible depending on the volume fraction of fibers present. Some of these are discussed below and they are applicable to both the hexagonal and the rectangular arrays.

Mode 1. This mode is possible when an inclined strip of thickness hl (Fig. 5a) can be drawn through the matrix without cutting any fiber. The assumed collapse velocity field is compatible and corresponds to a rigid body translation of the hatched areas parallel to themselves, and a uniform strain rate in the intervening matrix of $\epsilon_{11} = 0$, $\epsilon_{12} = \bar{\epsilon}_{12}/h$, $\epsilon_{13} = -(\bar{\epsilon}_{12}/h)\cot\theta$, $\epsilon_{23} = (\bar{\epsilon}_{22}/2h)\ (\tan\theta - \cot\theta)$, $\epsilon_{22} = -\epsilon_{33} = \bar{\epsilon}_{22}/h$ where $h = 1 - 2(a/l)\ \mathrm{cosec}\ \theta$.

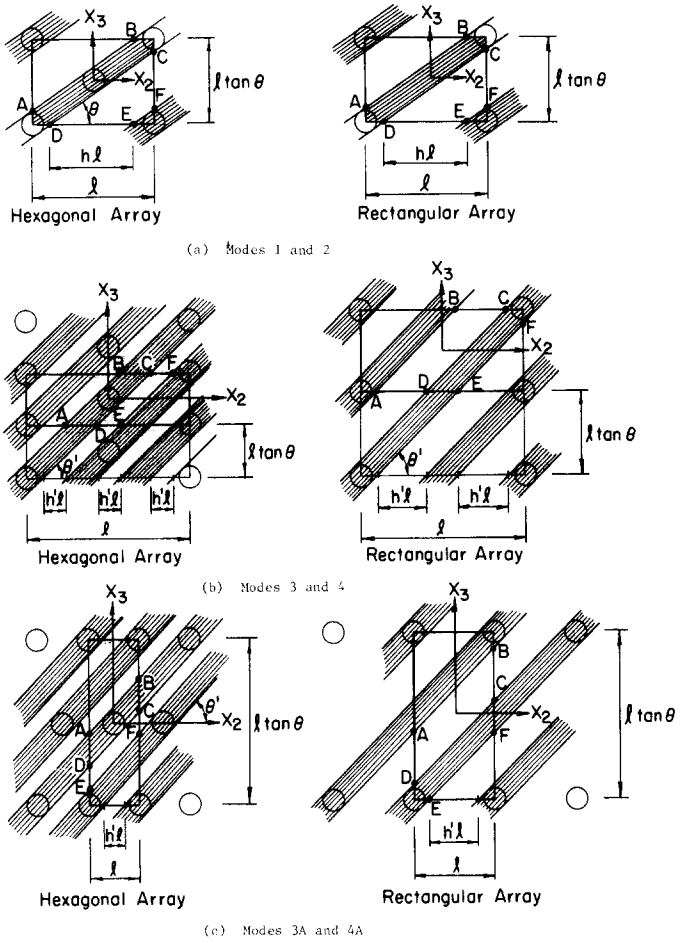

Fig. 5. Collapse modes for upper bound construction.

The upper bound for this assumed collapse field can be shown to reduce to

$$(\bar{\sigma}_{22}^{UB} \sin 2\theta)^2 + 4(\bar{\sigma}_{12}^{UB} \sin\theta)^2 = (2/\sqrt{3}\sigma_M)^2. \tag{3.12}$$

Notice that this upper bound is independent of h, which means that equation (3.12) gives an upper bound even when the strip width (hl) is reduced to zero.

Mode 2. If a uniform strain rate $\bar{\epsilon}_{11}$ (with $\epsilon_{22} = \epsilon_{33} = -1/2\bar{\epsilon}_{11}$) is superimposed on the strain rate field of Mode 1, then following the same procedure, an upper bound to the limit condition can be shown to be

$$(1/h^2)\,[\bar{\sigma}_{11}^{UB} - \tfrac{1}{2}\bar{\sigma}_{22}^{UB} - (\sigma_F v_F + \sigma_M v_M - \sigma_M h)]^2 + 3/4(\bar{\sigma}_{22}^{UB} \sin 2\theta)^2 + 3(\bar{\sigma}_{12}^{UB} \sin\theta)^2 = \sigma_M^2. \tag{3.13}$$

Mode 3. This mode is possible when a strip of thickness $h'l$ can be drawn at an angle θ' ($\theta' > \theta$) to the x_2 direction without cutting any fiber (Fig. 5b). This assumed collapse velocity field

corresponds to rigid body motions of the hatched areas parallel to themselves and a uniform strain rate in the remaining matrix of

$$\epsilon_{11} = 0, \epsilon_{12} = \bar{\epsilon}_{12}/\lambda h', \epsilon_{13} = -\bar{\epsilon}_{12}\cot\theta'/\lambda h', \epsilon_{22} = -\epsilon_{33} = \bar{\epsilon}_{22}/\lambda h'$$
$$\epsilon_{23} = 1/2\,\bar{\epsilon}_{22}(\tan\theta' - \cot\theta')/\lambda h'$$

where $\tan\theta' = \lambda\tan\theta$ and

$$\lambda = \begin{cases} 3 \text{ for hexagonal array} \\ 2 \text{ for rectangular array.} \end{cases}$$

Comparing this velocity field with that of Mode 1, it can immediately be concluded that the upper bound to the limit condition is

$$(\bar{\sigma}_{22}^{UB}\sin 2\theta')^2 + 4(\bar{\sigma}_{12}^{UB}\sin\theta')^2 = (2/\sqrt{3}\sigma_M)^2. \tag{3.14}$$

Mode 4. If a uniform strain rate $\bar{\epsilon}_{11}$ (with $\epsilon_{22} = \epsilon_{33} = -\frac{1}{2}\bar{\epsilon}_{11}$) is superimposed on Mode 3, then an upper bound to the limit condition can be shown to be

$$(1/\lambda h')^2[\bar{\sigma}_{11}^{UB} - 1/2\bar{\sigma}_{22}^{UB} - (\sigma_F v_F + \sigma_M v_M - \lambda h'\sigma_M)]^2 + 3/4(\bar{\sigma}_{22}^{UB}\sin 2\theta')^2 + 3(\bar{\sigma}_{12}^{UB}\sin\theta')^2 = \sigma_M^2 \tag{3.15}$$

where

$$\lambda h' = 1 - 2a/l[\lambda^2 + \cot^2\theta]^{1/2}.$$

Mode 3*A and* 4*A*. These modes are the same as Modes 3 and 4 with the difference that the angle θ' which the strip of thickness $h'l$ (Fig. 5c) makes with the x_2 axes is less than the angle θ of the array, and is given by

$$\tan\theta' = \frac{1}{\lambda}\tan\theta.$$

The form of the collapse velocity is the same and the final upper bound to the limit conditions have the same form as equations (3.14) and (3.15) however, the quantity $\lambda h'$ is now given by

$$\lambda h' = \lambda - 2(a/l)\,[\lambda^2 + \cot^2\theta]^{1/2}.$$

Mode 5. This mode is applicable whenever it is possible to pass a strip parallel to the $x_1 - x_3$ plane without cutting across a fiber (Fig. 6a). Notice that this is always possible for the rectangular array right up to the maximum volume fraction of fibers that can be put into the composite. The velocity field corresponds to rigid body motion of the hatched areas in the x_1 direction and a uniform shear strain rate in the remaining matrix of $\epsilon_{12} = \bar{\epsilon}_{12}/h_1$. The resulting upper bound is

$$\bar{\sigma}_{12}^{UB} = \sigma_M/\sqrt{3}. \tag{3.16}$$

Thus, whenever a plane can be passed parallel to the $x_1 - x_3$ plane without cutting a fiber, the upper bound to the shear strength of the composite is the matrix shear strength. Since this is also the lower bound to the shear strength of the composite (equation 3.8), it represents the exact limit strength in shear.

Mode 6. If a uniform strain rate in the x_1 direction is superimposed on the collapse field for Mode 5, then an upper bound to the shear strength becomes

$$(1/h_1)^2[\bar{\sigma}_{11}^{UB} - (\sigma_F v_F + \sigma_M v_M - \sigma_M h_1)]^2 + 3\bar{\sigma}_{12}^{UB^2} = \sigma_M^2. \tag{3.17}$$

$$h_1 = \begin{cases} 1 - 4(a/l) \text{ for hexagonal array} \\ 1 - 2(a/l) \text{ for rectangular array.} \end{cases}$$

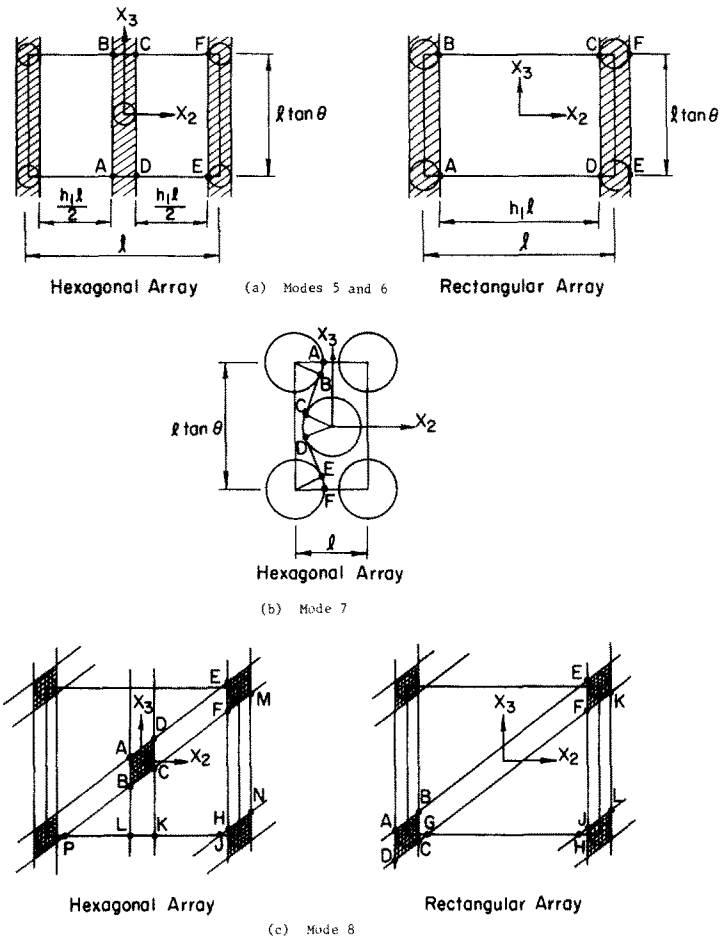

Fig. 6. Collapse modes for upper bound construction.

Mode 7. For the hexagonal array when the volume fraction is large [$v_F > (\pi/8)\cot\theta$], it is not possible to pass a plane parallel to the $x_1 - x_3$ plane without cutting across a fiber. In such cases Mode 5 is not applicable, but a good upper bound to the shear strength can be obtained by considering a discontinuous collapse field (Fig. 6b).

A line ABCDEF is drawn in the $x_2 - x_3$ plane such that BC and DE are straight lines tangential to the fibers, and curves AB, CD, EF are parts of the three fiber circumferences involved. A discontinuous velocity field is assumed such that

$$u_1 = u_2 = u_3 = 0 \text{ to the left of ABCDEF}$$

$$\left.\begin{aligned} u_1 &= u \\ u_2 &= u_3 = 0 \end{aligned}\right\} \text{to the right of ABCDEF.}$$

Considering the above collapse velocity field an upper bound to the in-plane shear strength of a hexagonal array of fibers is

$$\bar{\sigma}_{12}^{UB} = \begin{cases} \sigma_M/\sqrt{3} \text{ for } v_F \le (\pi/8)\cot\theta \\ \sigma_M/\sqrt{3}\{4a/l\cot\theta\,[\theta - \cos^{-1}(4a\cos\theta/l)] \\ +[\operatorname{cosec}^2\theta - 16a^2/l^2\cot^2\theta]^{1/2}\} \text{ for } v_F \ge (\pi/8)\cot\theta. \end{cases} \tag{3.18}$$

Notice that v_F is related to a/l by

$$a/l = [(v_F/2\pi)\tan\theta]^{1/2}.$$

For the rectangular array, the upper bound to the shear strength is always given by $\sigma_M/\sqrt{3}$, which as mentioned before, is the exact limit shear strength.

Mode 8. The collapse mode for this case is a combination of Mode 1 (with $\bar{\epsilon}_{12} = 0$) and Mode 5. This is applicable whenever both the vertical strip and the inclined strip can be drawn without cutting across a fiber (Fig. 6c). The corresponding upper bound becomes

$$(1/h_1^2)\,[\bar{\sigma}_{22}^{UB} \sin 2\theta - (2/\sqrt{3})\sigma_M(1-h_1)]^2 + (2/h)^2\,[\bar{\sigma}_{12}^{UB} - (\sigma_M/\sqrt{3})\,(1-h)]^2 = (2/\sqrt{3}\sigma_M)^2. \quad (3.19)$$

Other modes are possible for the periodic array of fibers, especially for low volume fraction of fibers. But the ones considered above have been found to give smaller upper bounds for the volume fractions and geometries considered. It should be noted that in all the modes considered (except Mode 7), the circular section of the fibers was not of any importance. These modes were based on passing planes through the composite without cutting across any fiber. Thus, as long as these planes can be drawn, these modes are applicable irrespective of the shape of the fiber cross-section. The range of applicability of these modes in terms of volume fraction of fibers will, of course, depend on the shape of the cross-section of the fibers. If the fiber cross-section is noncircular, a velocity field analogous to Mode 7 can be assumed depending on the exact shape of the cross-section of fibers and an upper bound can be derived in a similar fashion.

It should also be noted that Modes 1, 3, 3A and 4 are applicable as long as just one plane can be passed through the composite in certain directions without cutting any fiber and so these modes can tolerate some variation of the geometry from perfect periodicity, especially for low volume fraction of fibers. The rest of the modes depend on the width of strips that can be passed periodically through the composite without cutting any fiber. If departure from periodicity is restricted to small proportion of the composite, then these results should be more or less unaffected.

For the periodic arrays, the lower bounds to the composite limit condition have been computed according to equations (3.8) and (3.10) and are, therefore, independent of the type of array. The upper bounds, however, are computed by using the various modes discussed earlier and are, therefore, dependent on the type of array used. Table 2 gives the various geometry and volume fraction of fibers that have been considered for computation. The last column in Table 2 contains the maximum volume fraction of fibers which can exist for each particular type of array. The ratio between the uniaxial limit strengths of the fiber and the matrix has been assumed equal to 20 in all cases. Typical upper and lower bounds to the composite limit condition for the hexagonal arrays are shown for $(\bar{\sigma}_{11} - \bar{\sigma}_{22})$, $(\bar{\sigma}_{11} - \bar{\sigma}_{12})$ and $(\bar{\sigma}_{22} - \bar{\sigma}_{12})$ loadings in Figs. 7 and 8. The various parts of the upper bound surface correspond to the different mode shapes and are indicated on the figures. Upper and lower bounds for the rectangular arrays are very similar to those of the hexagonal arrays although the mode shapes for the upper bound are slightly different[9].

4. STRENGTH OF A COMPOSITE WITH THE FIBERS AT AN ANGLE TO x_1 AXIS

In all cases up to now the fiber axis has been taken in the x_1 direction. If the fibers were instead at an angle ϕ with the x_1 axis, and the RVE is subjected to general loading $\bar{\sigma}_{\alpha\beta}$, the limit strength will obviously depend very strongly on the angle ϕ. The limit stresses in this case can be obtained by noting that in a (x_1', x_2', x_3') system where x_1' is in the direction of the fiber axis, the stresses corresponding to $\bar{\sigma}_{\alpha\beta}$ are

$$\bar{\sigma}_{11}' = \bar{\sigma}_{11}\cos^2\phi + \bar{\sigma}_{22}\sin^2\phi + \bar{\sigma}_{12}\sin 2\phi$$

$$\bar{\sigma}_{22}' = \bar{\sigma}_{11}\sin^2\phi + \bar{\sigma}_{22}\cos^2\phi - \bar{\sigma}_{12}\sin 2\phi$$

$$\bar{\sigma}_{12}' = (1/2)(\bar{\sigma}_{22} - \bar{\sigma}_{11})\sin 2\phi + \bar{\sigma}_{12}\cos 2\phi.$$

Since the limit condition (or bounds to it) have been computed for the primed system, these together with the above equations enable the computation of the total limit surface (or bounds to it) for any angle of fiber orientation with respect to x_1 axis.

Of considerable practical importance is the variation of uniaxial tensile strength with the angle

Table 2. Geometry of periodic array

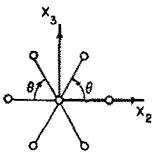

Hexagonal Array

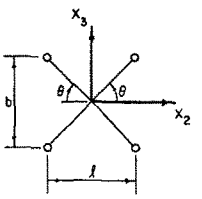

Rectangular Array

Type of Array	θ or b/ℓ	v_F	$v_{F_{max}}$
Hexagonal	30°	.1 .3 .5	.91
	45°	.1 .3 .5	.7854
	60	.1 .3 .5	.91
Rectangular	b/ℓ = 1/2	.1 .3	.39
	b/ℓ = 1	.1 .3	.7854
	b/ℓ = 2	.1 .3	.39

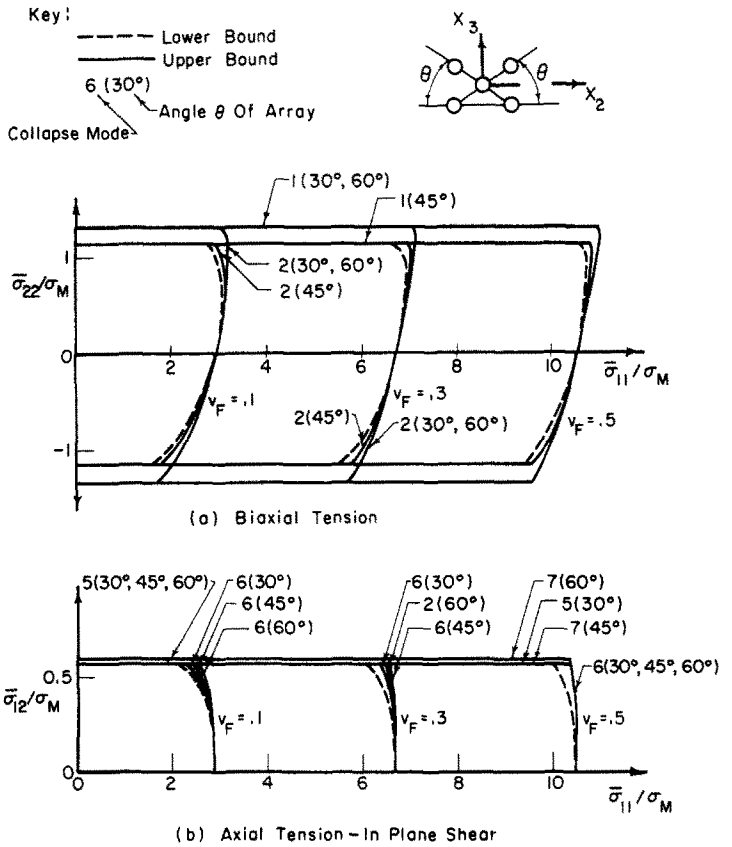

Fig. 7. Upper and lower bounds for hexagonal arrays ($\sigma_F/\sigma_M = 20$).

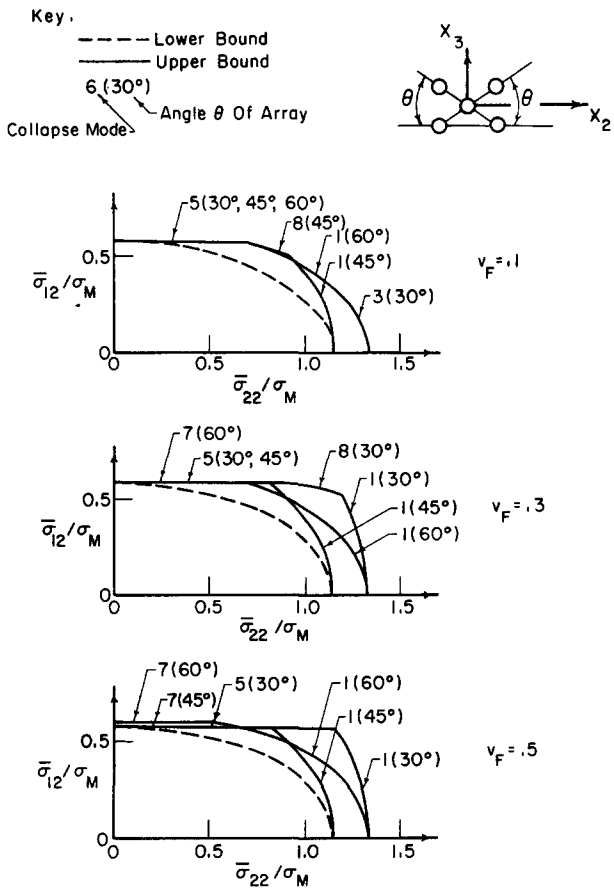

Fig. 8. Upper and lower bounds for hexagonal arrays in transverse tension-in plane shear loading.

ϕ that the fibers make with the direction of pull. Figure 9 shows plots of bounds to the uniaxial tensile limit strength for various angles of the fiber axis with the x_1 direction and for three types of hexagonal array of fiber distribution. The bounds are close for all angles of fiber orientation. For cases where the fibers are close to 90° with the x_1 axis, the upper bound corresponds to Mode 1. For intermediate angles (25° – 55°), the upper bound corresponds to the shear Mode 7. When the fibers are at a shallow angle with the x_1 axis, the upper bound corresponds to Mode 2 or 6 which involve plastic flow of the fibers. Though the mode shapes assumed for upper bound analysis are not necessarily the true collapse modes, it is interesting to note that these are the three modes of failure observed by Jackson and Cratchley[17] in their tests with composites made of aluminium matrix reinforced by 50 per cent volume fraction of unidirectional silica fibers. Their test data are included in these plots, the arrows indicating corrections needed for fiber axis reorientation and specimen damage during testing. Figure 9 also shows a similar plot for the random composite cylinder assembly[18, 9]. Except for angles of fiber orientation close to 90°, the data from Jackson and Cratchley[17] seem to fit these results quite well. Since the results for the periodic array are quite close to those of the random composite cylinder assembly, the fiber distribution geometry does not affect the uniaxial limit strength of undirectional fiber-reinforced composites appreciably except at angles of orientation of the fibers near 90° with the direction of loading.

5. CONCLUSIONS

Upper and lower bounds to the uniaxial fiber-reinforced composite plane stress limit conditions have been obtained for various phase geometries and volume fractions. In general, the bounds can be brought closer together by incorporating more geometrical data into the analysis.

Procedures for obtaining general upper and lower bounds to the composite limit condition are given. They are applicable for arbitrary fiber cross-section and distribution, and for cases where the fiber and matrix obey different limit conditions. The general upper bound has been shown to

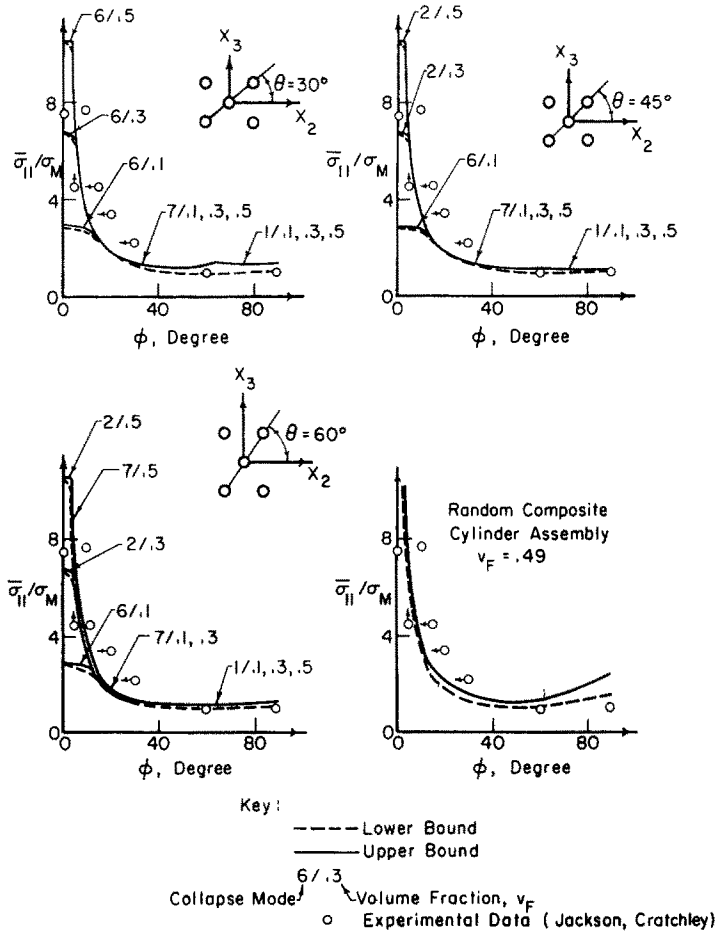

Fig. 9. Uniaxial limit strengths for various fiber orientations and arrays.

be the best possible upper bound from a knowledge of volume fractions of phases alone. Similar conclusions can be drawn for the general lower bound only for the axial and transverse tension and in-plane shear loadings.

When the fiber cross-sections are arbitrarily distributed but are known to be circular with arbitrary radius, the upper bound to the in-plane shear strength of the composite can be significantly improved over the more general results. The general lower bounds to axial and transverse tensions and in-plane shear strengths which are applicable to this case can be shown to be the best possible lower bounds from a knowledge of volume fraction and circular cross-sectional shape of the fibers for all volume fraction of fibers. Using circular section fibers of arbitrary radius and distribution, the in-plane shear strength of a composite can at most be increased by 27 per cent over the matrix strength irrespective of the fiber strength.

The upper bound to the composite limit condition can be further improved for the cases where the fibers are distributed in a periodic array. The difference between these upper bounds and the general lower bound for arbitrary fiber cross-section and location are, in general, small compared to the axial tensile strength of the composite. The difference is largest for the combined transverse tension and in-plane shear loading and when viewed as fraction of the matrix strength. For combined axial and transverse tension, and combined axial tension-shear loadings the limit conditions are mainly controlled by the volume fraction and strengths of the phases and are insensitive to the types of array considered. The limit condition for the combined transverse tension-shear loading, however, varies little with volume fractions or type of array for small to moderate fiber volume fractions. For high volume fractions of fibers, the transverse strength of the composite should increase with volume fraction.

The uniaxial limit strength for the case where the fibers are at an angle to the direction of loading are found to be insensitive to the way fibers are distributed. For shallow angles to the

fiber direction, the volume fraction and the strengths of the phases determine the tensile strength of the composite. For larger angles, the composite tensile strength is controlled by the strength of the matrix.

REFERENCES

1. D. C. Drucker, *On Minimum Weight Design and Strength of Non-homogeneous Plastic Bodies, Non-homogeneity in Elasticity and Plasticity* (Edited by W. Olszak) p. 139. Pergamon Press, New York (1959).
2. Z. Hashin, Transverse Strength of Fibrous Composites. Evaluation of Filament Reinforced Composites for Aerospace Structural Applications, NASA CR-207 (1965).
3. D. C. Drucker, Engineering and continuum aspects of high strength materials, high strength materials. *Proc. 2nd Berkely Int. Mater. Conf.* (Edited by V. F. Zackay) p. 795. Wiley, New York (1965).
4. T. W. Butler and E. J. Sullivan, Jr., On the transverse strength of fiber reinforced materials. *J. Appl. Mech.* **40**, 523 (1973).
5. L. S. Shu and B. W. Rosen, Strength of fiber-reinforced composites by limit analysis methods. *J. Composite Mater.* **1**, 366–381 (1967).
6. W. Prager, Plastic failure of fiber reinforced materials. *J. Appl. Mech.* **36**, 542–544 (1969).
7. J. D. Helfinstine and R. H. Lance, Yielding of a Fiber-Reinforced Tresca Material, presented at ASCE-EMD Specialty Conference, Mechanics Research in Civil Engineering, University of Illinois at Urbana-Champaign (1971).
8. P. V. McLaughlin, Plastic limit behavior and failure of filament-reinforced materials. *Int. J. Solids Structures* **8**, 1299–1318 (1972).
9. S. Majumdar, Plastic Limit Strength of Unidirectional Fiber-Reinforced Composites, Thesis submitted in partial fulfillment of the requirements for the degree of Doctor of Philosophy in Theoretical and Applied Mechanics, University of Illinois, Urbana (1973).
10. S. Majumdar and P. V. McLaughlin, Jr., Application of Limit Analysis to Composite Materials and Structures, Presented at the Seventh U.S. National Congress of Applied Mechanics, June 3–7, 1974, Boulder, Colorado. *J. Applied Mechanics* **41**, 995 (1974).
11. D. C. Drucker, W. Prager and H. J. Greenberg, Extended limit design theorems for continuous media. *Q. Appl. Math.* **9**, 381–389 (1952).
12. H. L. Frisch, Statistics of random media. *Trans. Soc. Rheology* **9**, 293–312 (1965).
13. Z. Hashin, On elastic behavior of fiber-reinforced materials of arbitrary transverse phase geometry. *J. Mech. Phys. Solids* **13**, 119–134 (1965).
14. M. J. Beran and J. M. Molyneux, Use of classical variational principles to determine bounds for the effective bulk modulus in heterogeneous media. *Q. Appl. Math.* **24**, p. 108 (1966).
15. Z. Hashin, *Theory of Composite Materials.* Towne School, University of Pennsylvania, Pa. (1967).
16. S. Majumdar and P. V. McLaughlin, Jr., Upper Bounds to in-plane shear strength of unidirectional fiber-reinforced composites. *J. Appl. Mech.* **40**, 824–825 (1973).
17. P. W. Jackson and D. Cratchley, The effect of fiber orientation on the tensile strength of fiber-reinforced metals. *J. Mech. Phys. Solids* **14**, 49–64 (1966).
18. Z. Hashin and B. W. Rosen, The elastic modulii of fiber-reinforced materials. *J. Appl. Mech.* **31**, 223–232 (1964).